Supplementary Information

De novo post-SELEX optimization of a G-quadruplex DNA aptamer binding to marine toxin gonyautoxin 1/4

Menghua Song[a,†], Gan Li[a,†], Qi Zhang[a,†], Jianping Liu[a,*] and Qiang Huang[a,b,*]

[a]*State Key Laboratory of Genetic Engineering, Shanghai Engineering Research Center of Industrial Microorganisms, MOE Engineering Research Center of Gene Technology, School of Life Sciences, Fudan University, Shanghai 200438, China*

[b]*Multiscale Research Institute of Complex Systems, Fudan University, Shanghai 201203, China*

[†]These first three authors contributed equally to this work.

*Corresponding authors. Email address: huangqiang@fudan.edu.cn (Q. Huang), jpliu@fudan.edu.cn (J. Liu)

Figures

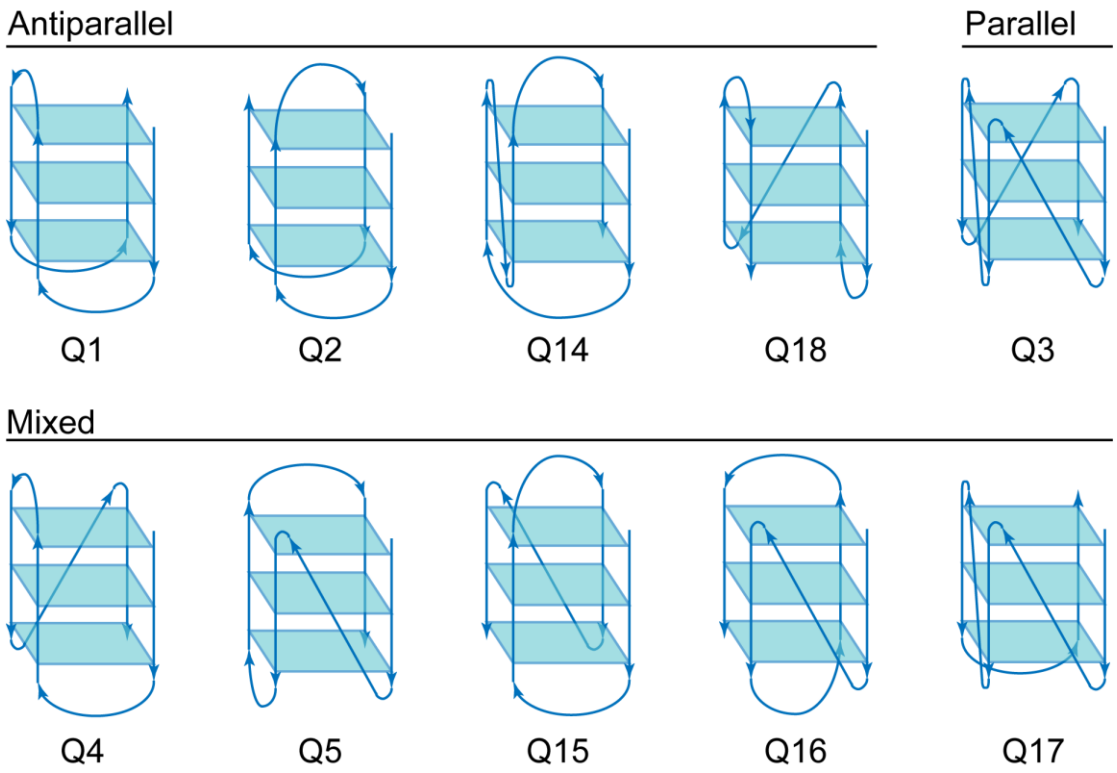

Fig. S1. Strand orientation in different GQ types. Q1, Q2, Q14 and Q18 are antiparallel types; Q3 is parallel type; Q4, Q5, Q15, Q16 and Q17 are mixed types.

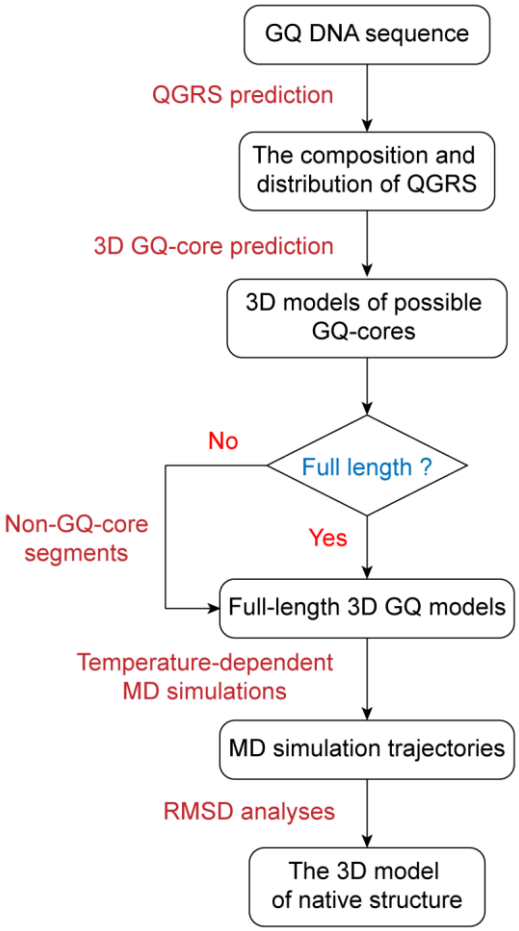

Fig. S2. 3D structure prediction pipeline of GQ aptamers. QGRS prediction is performed via the QGRS Mapper web server (http://bioinformatics.ramapo.edu/QGRS/analyze.php). 3D GQ-core models are predicted with the G-Quadruplex module of the 3D-Nus web server (https://www.iith.ac.in/3dnus/Quadruplex.html). Non-GQ-core segments are extended with the AutoPSF VMD plugin (https://www.ks.uiuc.edu/Research/vmd/).

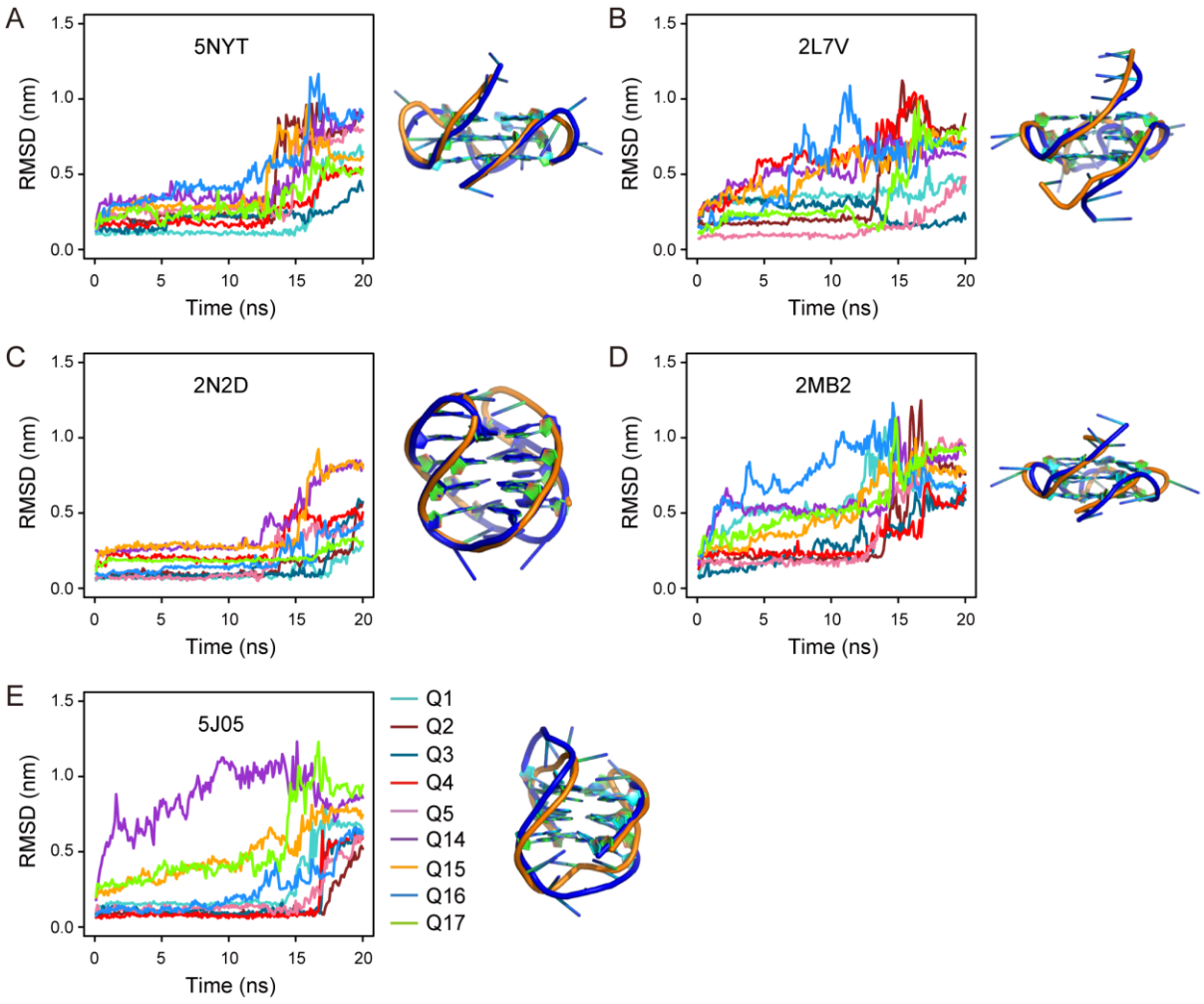

Fig. S3. Time-dependent RMSDs of the G-tetrad guanines in the TdMD simulations. PDB IDs of the experimental structures of GQ aptamers are given as: **(A)** 5NYT [1], **(B)** 2L7V [2], **(C)** 2N2D [3], **(D)** 2MB2 [4] and **(E)** 5J05 [5]. The experimental structures are shown in orange, and corresponding predicted structures in blue. For each simulation, the initial structure of the given aptamer is the reference of the RMSD calculations.

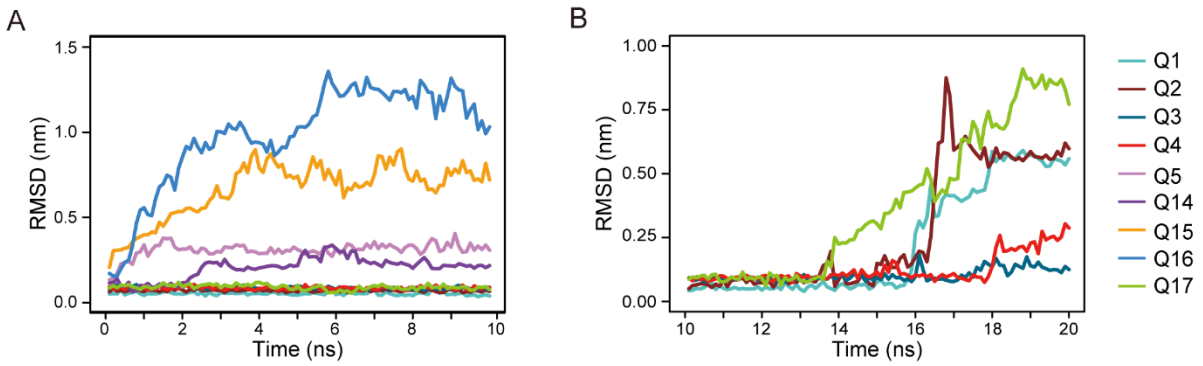

Fig. S4. RMSD analyses for the possible full-length models of GO18-T-d. **(A)** Time-dependent RMSDs of 8 G-tetrad guanines in the constant-temperature MD simulations. **(B)** Time-dependent RMSDs of 8 G-tetrad guanines in the heating simulations. For each simulation, the initial structure of the given aptamer is the reference of the RMSD calculations.

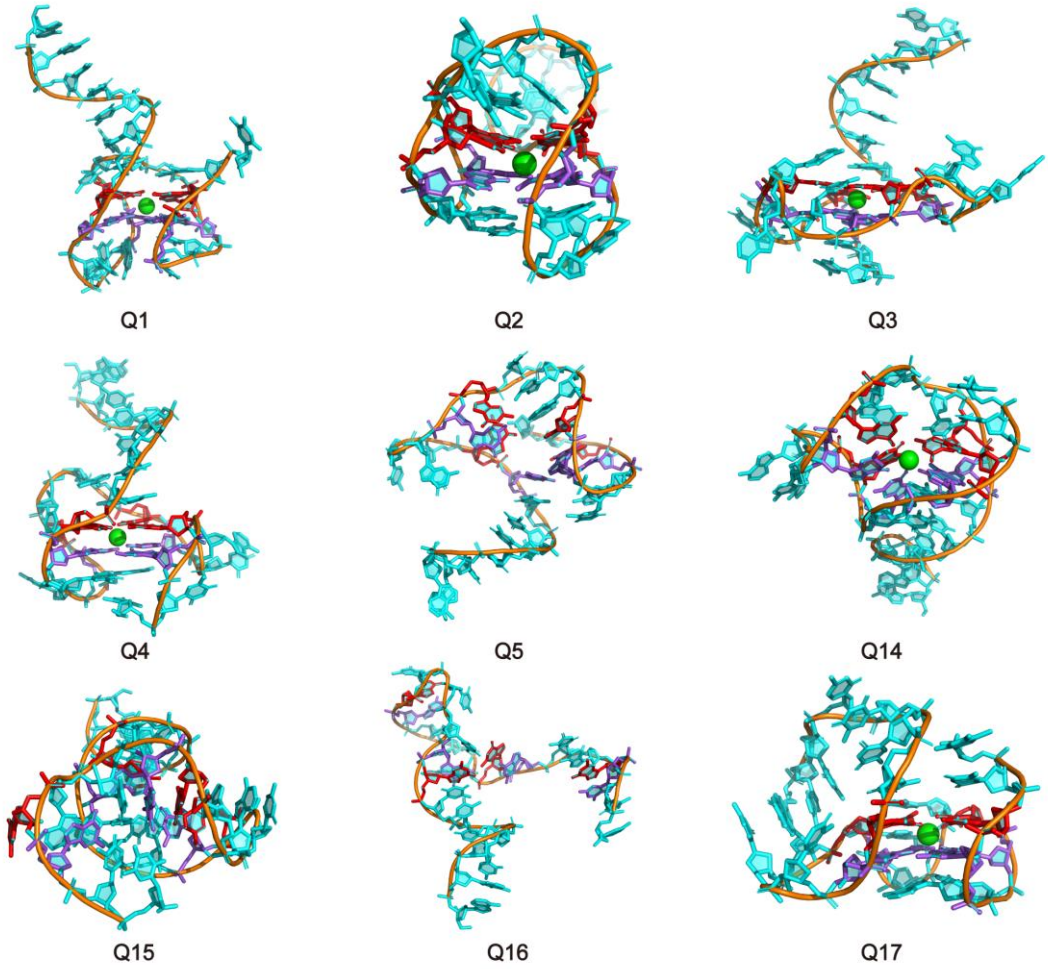

Fig. S5. MD conformations of the GO18-T-d models at the end of the constant-temperature simulations. The aptamer is shown as cartoon and sticks in cyan, the G-tetrads as cartoon and sticks in red/purple, and Mg^{2+} as spheres in green.

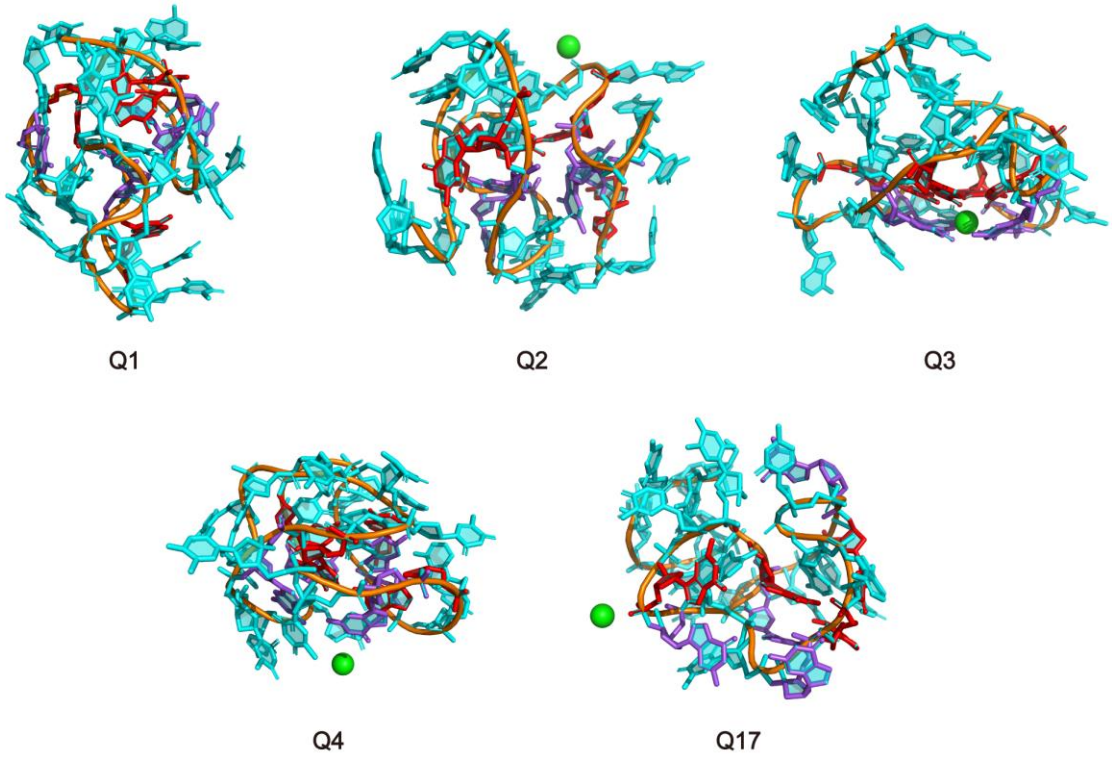

Fig. S6. MD conformations of the GO18-T-d models at the end of the heating simulations. The aptamer is shown as cartoon and sticks in cyan, the G-tetrads as cartoon and sticks in red/purple, and Mg^{2+} as spheres in green.

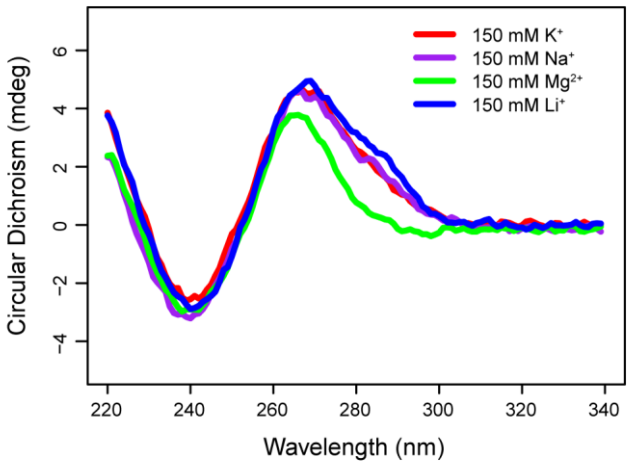

Fig. S7. CD spectra of GO18-T-d in the presence of different cations. The aptamer was annealed directly in the buffers (20 mM Tris-HCl, pH 7.4) with ions.

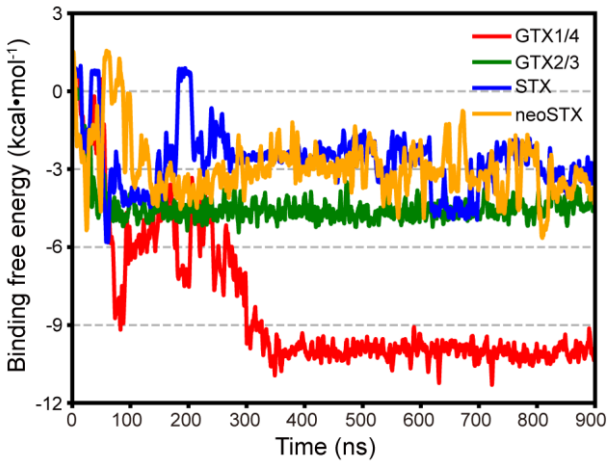

Fig. S8. Time-dependent binding free energies of GO18-T-d in complex with different toxins (red: GTX1/4, green: GTX2/3, blue: STX, orange: neoSTX).

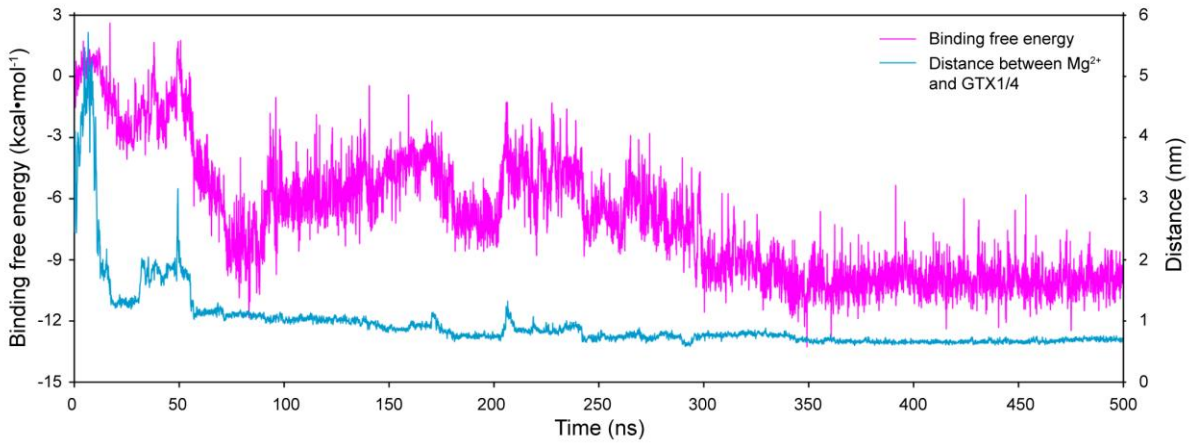

Fig. S9. Time-dependent binding free energy and distance between the center of GTX1/4 and Mg^{2+} in the center of GQ-core.

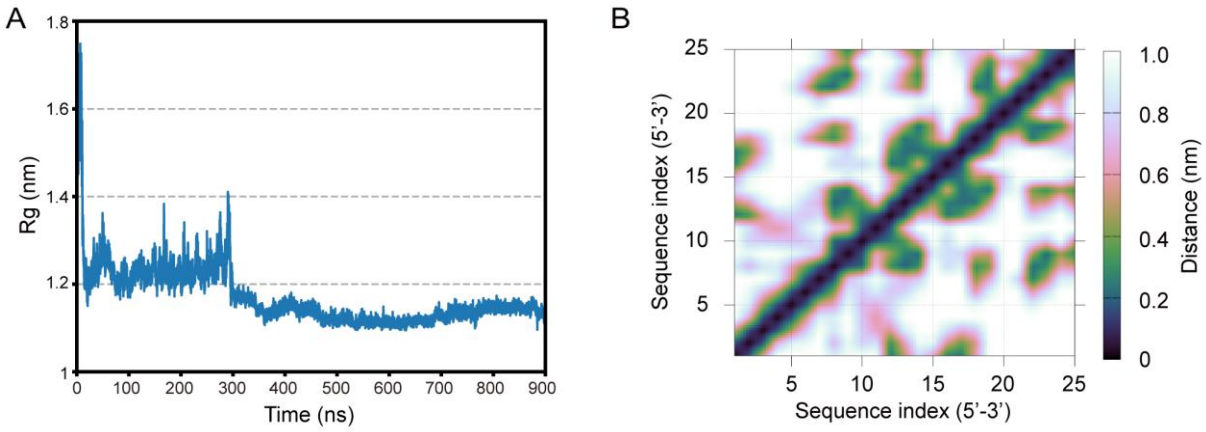

Fig. S10. (A) Time-dependent gyration radius (Rg) of GO18-T-d:GTX1/4. (B) The contact map of GO18-T-d in the GO18-T-d:GTX1/4 system.

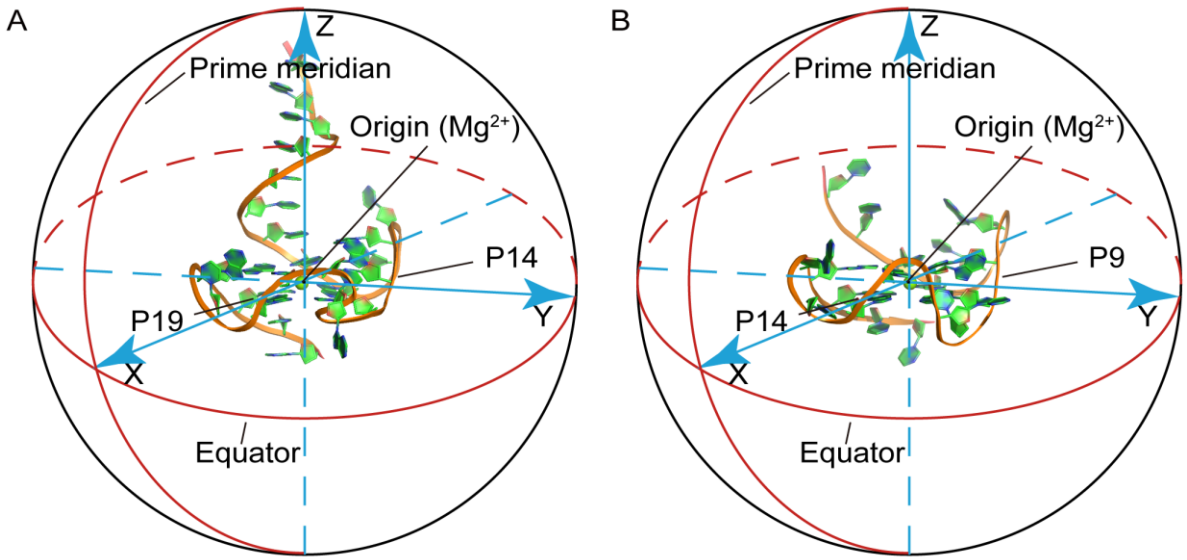

Fig. S11. The spherical coordinate system for constructing the binding free energy landscapes of **(A)** GO18-T-d and **(B)** tGO18-T-d.

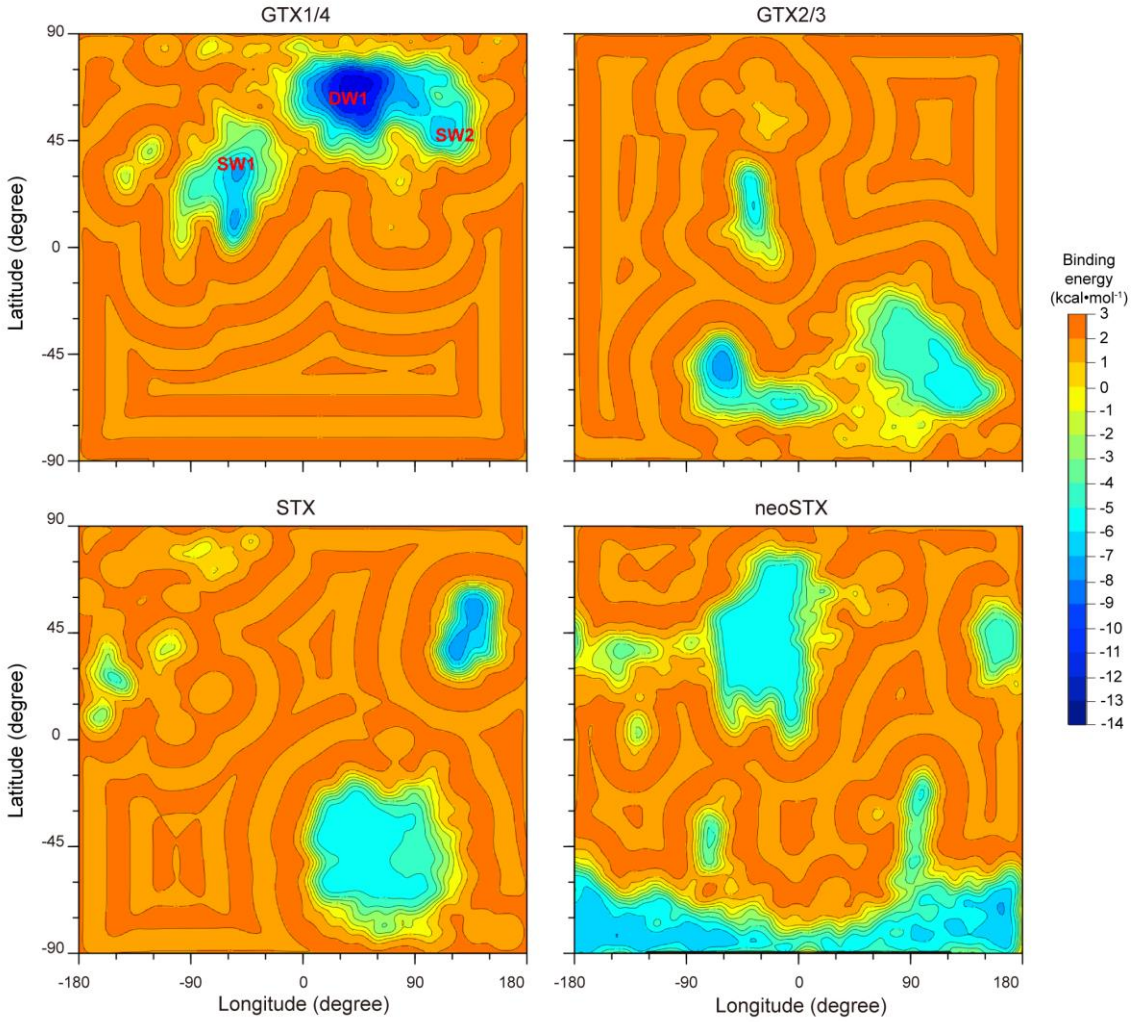

Fig. S12. The binding energy landscape of four toxin:GO18-T-d systems.

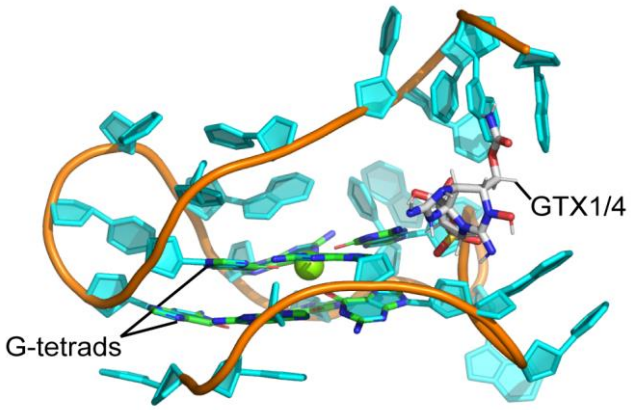

Fig. S13. A representative complex structure that illustrates the 5'-end of GO18-T-d hampers the entry of GTX1/4 into the binding pocket of GO18-T-d.

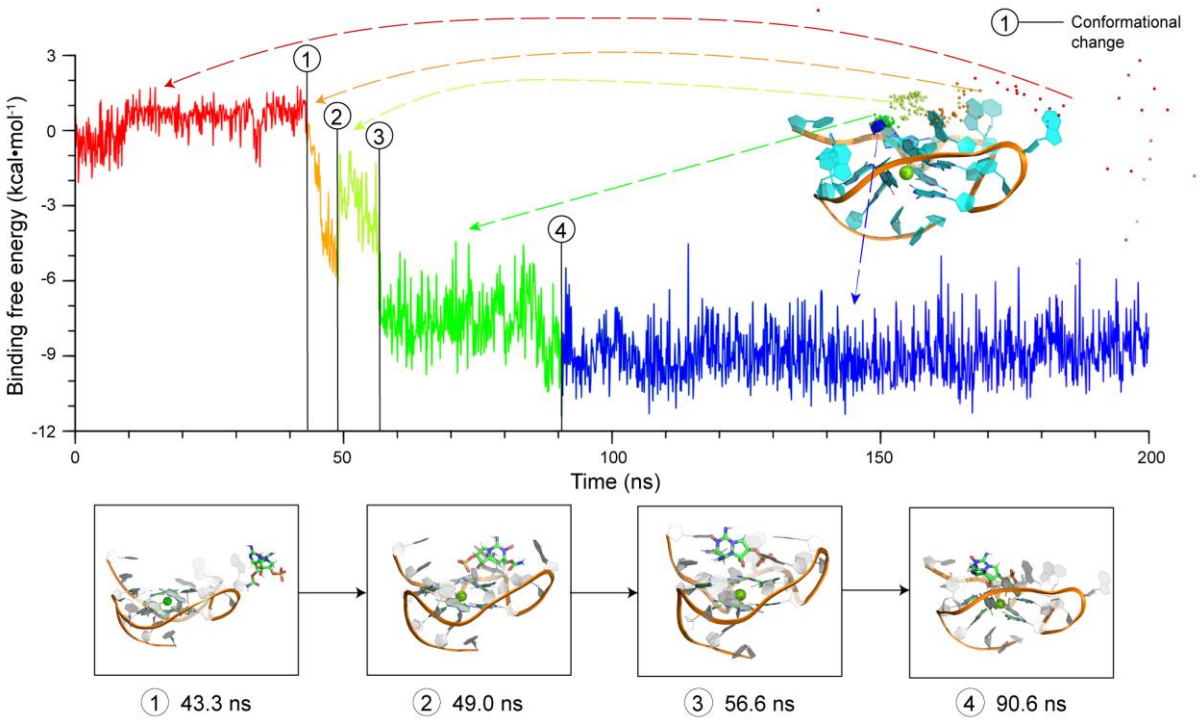

Fig. S14. Spontaneous association of GTX1/4 with tGO18-T-d. Time-dependent binding free energies of the tGO18-T-d:GTX1/4 complex, and corresponding positions of the center of mass of GTX1/4 (spheres in rainbow colors) on tGO18-T-d. Four representative conformational changes are given in the panels below. Corresponding movie showing the spontaneous association process is presented in Supplementary Movie S2.

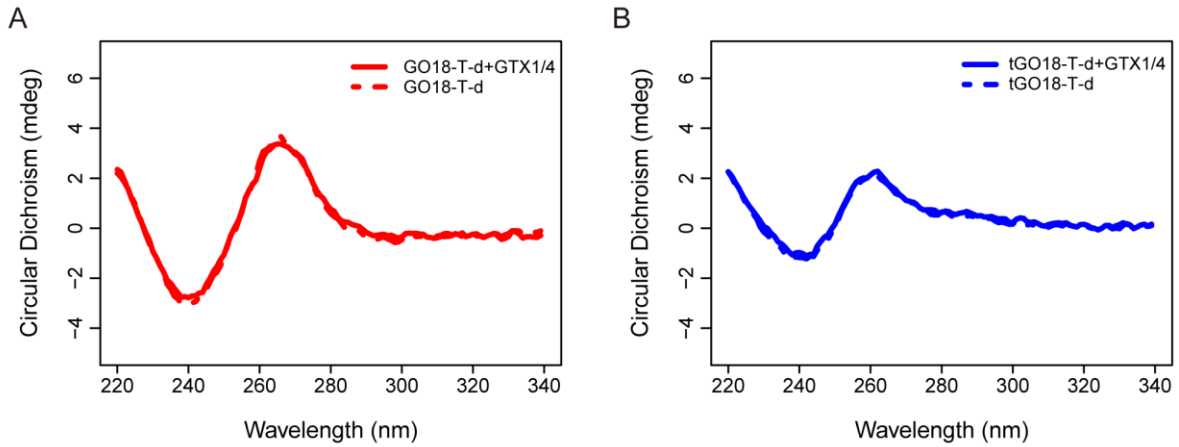

Fig. S15. CD spectra of GO18-T-d (A) and tGO18-T-d (B) in the presence (solid line) and absence (dash line) of GTX1/4 (1 μM). The aptamers (20 μM) were annealed directly in the buffer (20 mM Tris-HCl, pH 7.4) with 150 mM $MgCl_2$.

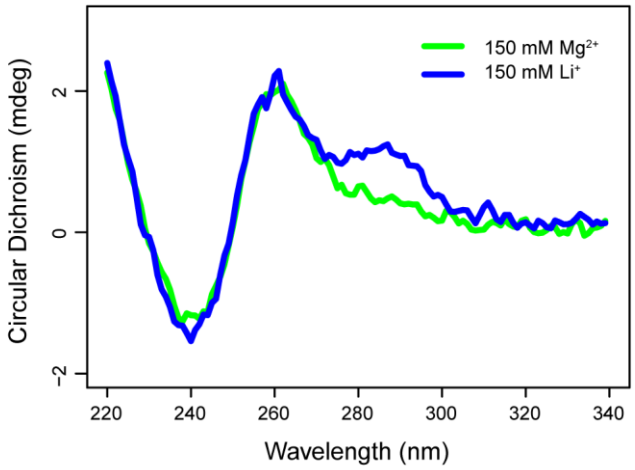

Fig. S16. CD spectra of tGO18-T-d in the presence of different cations. The aptamer was annealed directly in the buffers (20 mM Tris-HCl, pH 7.4) with ions.

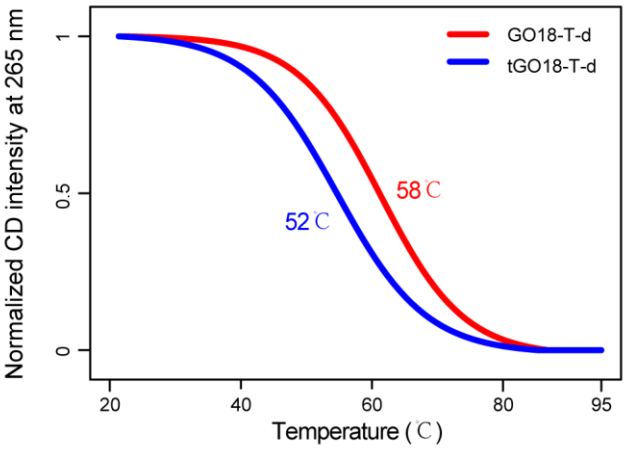

Fig. S17. Normalized CD intensity at 265 nm with increasing temperatures. The aptamers (20 μM) were annealed directly in the ionic buffer. The buffer is (20 mM Tris-HCl, pH 7.4) supplemented with 150 mM $MgCl_2$.

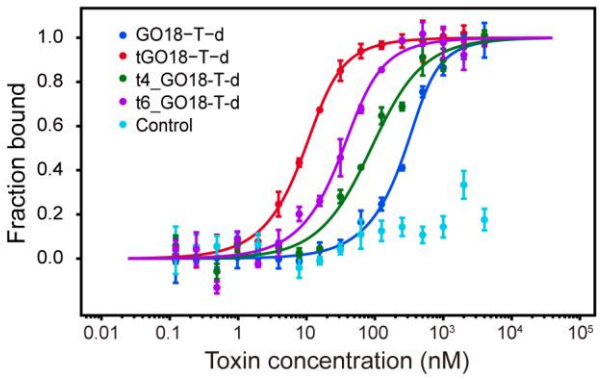

Fig. S18. MST experiments for GO18-T-d (blue), tGO18-T-d (red), t4_GO18-T-d (green), t6_GO18-T-d (purple) and Control (random sequence, cyan). The K_d values of GO18-T-d, tGO18-T-d, t4_GO18-T-d and t6_GO18-T-d are 75.63 ± 25.33 nM, 3.60 ± 0.67 nM, 68.66 ± 32.98 nM and 14.72 ± 10.02 nM, respectively. The control shows no binding affinity for GTX1/4.

Tables

Table S1. GQ aptamers for testing the structure prediction pipeline.

PDB ID	Sequence (5′-3′)	experimental type	Predicted type	RMSD value (Å)
5NYT	TAGGGACGGGCGGGCAGGGT	Q3	Q3	1.3
2L7V	TGAGGGTGGGTAGGGTGGGTAA	Q3	Q3	1.5
2N2D	GGGGCCGGGGCCGGGGCCGGGG	Q1	Q1	1.5
2MB2	TTGGGGGGGGGGGGGGGT	Q3	Q3	3.9
5J05	GGGTTTGGGTTTTGGGAGGG	Q2	Q2	4.0

Table S2. Nucleotide sequences of DNA aptamers used in MST and CD experiments.

Aptamer*	Length (-nt)	DNA Sequence (5′-3′)
GO18-T-d	25	AACCTTTGGTCGGGCAAGGTAGGTT
tGO18-T-d	20	TTGGTCGGGCAAGGTAGGTT
t4_GO18-T-d	21	TTTGGTCGGGCAAGGTAGGTT
t6_GO18-T-d	19	TGGTCGGGCAAGGTAGGTT
Control	25	TCACGAACTTCATTAACTGACTTAC

* Each sequence was labeled with 6-FAM at its 3'-end.

Movies

Movie S1. The spontaneous association of GTX1/4 with GO18-T-d. For the sake of clarity, water molecules, ions in the solvent and hydrogen atoms of GO18-T-d are not shown. In the movie, GO18-T-d is shown as cartoon in cyan, GTX1/4 as spheres and sticks in green, and Mg^{2+} as spheres in green.

Movie S2. The spontaneous association of GTX1/4with tGO18-T-d. For the sake of clarity, water molecules, ions in the solvent and hydrogen atoms of tGO18-T-d are not shown. In the movie, tGO18-T-d is shown as cartoon in cyan, GTX1/4 as spheres and sticks in green, and Mg^{2+} as spheres in green.

Reference

1. Trajkovski M, Endoh T, Tateishi-Karimata H, Ohyama T, Tanaka S et al. (2018) Pursuing origins of (poly)ethylene glycol-induced G-quadruplex structural modulations. *Nucleic Acids Res* 46: 4301-4315.
2. Dai J, Carver M, Hurley LH, Yang D (2011) Solution structure of a 2:1 quindoline-c-MYC G-quadruplex: insights into G-quadruplex-interactive small molecule drug design. *J Am Chem Soc* 133: 17673-17680.
3. Brcic J, Plavec J (2015) Solution structure of a DNA quadruplex containing ALS and FTD related GGGGCC repeat stabilized by 8-bromodeoxyguanosine substitution. *Nucleic Acids Res* 43: 8590-8600.
4. Sengar A, Heddi B, Phan AT (2014) Formation of G-quadruplexes in poly-G sequences: structure of a propeller-type parallel-stranded G-quadruplex formed by a G_{15} stretch. *Biochemistry* 53: 7718-7723.
5. Dvorkin SA, Karsisiotis AI, Webba da Silva M (2018) Encoding canonical DNA quadruplex structure. *Sci Adv* 4: eaat3007.